Aqua regia activated Au/C catalysts for the hydrochlorination of acetylene

Marco Conte,[a,*] Catherine J. Davies,[a] David J. Morgan,[a] Thomas E. Davies,[a] David J. Elias,[a] Albert F. Carley,[a] Peter Johnston,[b] and Graham J. Hutchings [a,*]

[a] Cardiff Catalysis Institute, School of Chemistry, Cardiff University, Cardiff, CF10 3AT, UK

[b] Johnson Matthey Catalysts, Orchard Road, Royston, Herts, SG8 5HE, UK

*E-mail: ConteM1@cardiff.ac.uk, Hutch@cardiff.ac.uk

Abstract

Au/C catalysts are effective materials for the gas phase hydrochlorination of acetylene to vinyl chloride monomer, and to date, the most effective catalyst preparation protocol make use of impregnation using *aqua regia*. In the present study, the effect of this solvent is evaluated and discussed in detail by modifying the ratio of HCl and HNO_3 and the temperature of the impregnation step. These factors are observed to affect the Au^{3+}/Au^0 ratio of the final catalyst, in addition to the modification of the functional groups of the carbon used as support. The results can be rationalized by the oxidation effect of HNO_3 on both the gold nanoparticles and the functional groups on the carbon surface, as well as a nucleation effect of HCl towards gold over the carbon support. Kinetic parameters for the reduction of Au^{3+} to Au^0 were also determined and these support the existence of a redox cycle between Au^{3+}/Au^0 that could explain the overall catalytic activity.

Keywords: aqua regia, gold, carbon, acetylene hydrochlorination

1. Introduction

The manufacture of vinyl chloride monomer (VCM) is an essential chemical process with an average VCM production around 30 million tons per year [1] and it is primarily used as building block of poly-vinyl chloride The reaction is industrially carried out either *via* an oxychlorination reaction using ethylene as a substrate [2, 3], or *via* hydrochlorination of acetylene, by means of supported chloride catalysts, mainly mercuric chloride supported on carbon [4-6]. Due to a renewed interest in coal as derived feedstock the latter route has returned to being economically advantageous. However, the industrial catalysts based on mercuric chloride for the hydroclorination route have relatively short life time, due to the volatility of mercuric chloride, which presents clear environmental concerns. In contrast, Au^{3+} was postulated, and demonstrated, to be the most active catalyst for the hydrochlorination of acetylene [7, 8]. Previous studies have shown that the reaction occurs *via* the formation of a C_2H_2/Au/HCl complex [9, 10] with an activation effect by HCl and a detrimental effect by C_2H_2 on the catalyst performance during on stream studies. The catalysts are also affected by a slow deactivation [11], and this was found to be due to the reduction of Au^{3+} to Au^0 during the reaction. On-stream studies showed that it is possible to regenerate the catalyst by means of Cl_2 and NO [12]. On the other hand, it was possible to demonstrate that an off-line treatment that involves boiling the catalyst in *aqua regia* was an effective regeneration method [13], and at present it appears that *aqua regia* is also the best solvent for the preparation of this catalyst. This prompted us to investigate the catalyst preparation process in detail, with the aim of identifying the key factors enabling enhanced activity, and hence to determine what is so particular in the HCl:HNO_3 mixture used during the preparation process. The chemistry and the effects of *aqua regia* on either metal nanoparticles or carbon, is an area that has received virtually no attention to date, despite the vast use of metal based nanoparticles deposited on carbon [14-17] as the role of this solvent has been limited to a mere dissolving agent. On the contrary *aqua regia* is a complex mixture for which the generation and formation of native NOCl, Cl_2 and NO_x is still not well understood, and that could have serious implications in the preparation of catalytic materials, as in the case that is investigated and reported here. In addition, the nucleation process of Au^{3+} on carbon matrixes from chlorinated precursors such as $HAuCl_4$, is likely to be similar to that of widely used catalysts comprising Pd and Pt,

prepared from H_2PdCl_4 and H_2PtCl_4 respectively [18, 19], and consequently implications could be expected for reactions other than hydrochlorination e.g. partial oxidation of alcohols [20-22] and hydrocarbons [23-25]. In this way we anticipate that this work may have a wider relevance to catalyst design for such reactions.

2. Experimental

2.1 Catalyst preparation

All the catalysts were prepared by a wet impregnation method. The gold precursor, $HAuCl_4 \cdot xH_2O$ (Alfa Aesar, 40 mg, assay 49%) was dissolved in *aqua regia* (3:1 HCl (Fisher, 32%) : HNO_3 (Fisher, 70%) by volume, 5.4 ml) and the solution added dropwise with stirring to the activated carbon support (Norit ROX 0.8) (1.98 g) in order to obtain a catalyst with a final metal loading of 1% wt. Stirring was continued at ambient temperature until NO_x production subsided, approximately 10 minutes. The product was dried for 16 h at 110 °C and used as a catalyst. Variations to this protocol were introduced by changing drying temperature, (110, 140 and 185 ^oC), and the ratio of HCl and HNO_3 which was varied from 1:10 to 10:1. Catalysts including acid pre-treated carbons, were prepared in an identical manner than the impregnated samples but without initially adding the $HAuCl_4$ precursor.

2.2 Catalytic tests and characterization of the products

Catalysts were tested for acetylene hydrochlorination in a fixed-bed glass microreactor. Acetylene (5 mL min^{-1}, 0.5 bar) and hydrogen chloride (6 mL min^{-1}, 1 bar) were fed though a mixing vessel and preheater (70 ^oC), and further mixed in a N_2 flow (10 mL min^{-1}, 1 bar) *via* calibrated mass flow controllers to a heated glass reactor containing catalyst (200 mg), with a total GHSV of 740 h^{-1}. A reaction temperature of 180 ^{o} C was chosen, and blank tests using an empty reactor filled with quartz wool did not reveal any catalytic activity, even at 250 ^{o} C with the reactants under these flow conditions, SiC (2 x 2.5g) was used to extend the bed length, above and below the catalyst itself, separated by quartz wool. The pressure of the reactants, HCl, C_2H_2 and N_2, was chosen both for safety reasons and to test the catalyst under

mild conditions. As the VCM product is a class A carcinogen, and HCl as a gas can be corrosive, the time on-stream experimentation was fixed at 300 min (5h) as a maximum time. This was due to the trapping and venting capability of both HCl and VCM with the equipment in use and safety regulations in place at the laboratories where the experiments were performed. On an exceptional basis, a single 12 h test only was carried out in order to ascertain if the catalyst reached steady state conditions. The gas phase products were analyzed on-line by GC using a Varian 450GC equipped with a flame ionisation detector (FID). Chromatographic separation and identification of the products was carried out using a Porapak N packed column (6 ft x 1/8" stainless steel).

2.2.1 Reactor model and nature of the products

To combine the common use terms in the field of laboratory practice (i.e. the use of conversion in percentages) and the more appropriate description of the results in a industrial/engineering context (i.e. the use of productivity), we present conversion values in percentage in the manuscript but we replicate the data in full as productivities in the supplementary data. 100 % C_2H_2 conversion gives a VCM productivity of 80.7 mol kg_{cat}^{-1} h^{-1} under the reaction conditions we are using, due to the low values of GHSV and C_2H_2 concentration, we consider that we can approximate the reactor used to a differential reactor model. It is also important to note that the reactor feeding parameters, as well as the size of the catalytic bed, are constrained by the trapping and venting capability of HCl and VCM.

2.3 Characterization of the catalysts

2.3.1 *X-ray powder diffraction*

X-ray powder diffraction spectra (XRPD) were acquired using a X'Pert PanAlytical diffractometer operating at 40 kV and 40 mA selecting the Cu K_α radiation. Analysis of the spectra was carried out using X'Pert HighScore Plus software. Particle size was determined using the Scherrer equation [26] assuming spherical particles shapes and a K factor of 0.89. The line broadening was determined using a Voigt profile function

[27] convoluting the Gaussian and Lorentzian profile part of the reflection peak and the instrumental broadening for the Bragg-Brentano geometry used was estimated to be 0.06^{o} 2θ.

2.3.2 *X-ray photoelectron spectroscopy*

X-ray photoelectron spectroscopy (XPS) was performed with a Kratos Axis Ultra DLD spectrometer using a monochromatised AlK_{α} X-ray source (120 W) with an analyzer pass energy of 160 eV for survey scans and 40 eV for detailed elemental scans. Binding energies are referenced to the C(1s) binding energy of carbon, taken to be 284.7 eV.

2.3.3 Scanning electron microscopy

Scanning electron microscopy (SEM) and energy dispersive X-ray (EDX) analyses were performed using a Carl Zeiss EVO-40 microscope and Oxford instrument SiLi detector respectively. Samples were mounted on aluminium stubs using adhesive carbon discs. EDX data was averaged from multiple overscans and spot analysis is considered representative of the sample. SEM was used to analyse the morphology of the samples, while SEM-EDX to determine the chemical composition of the samples

2.3.4 Transmission electron microscopy

Samples were prepared for transmission electron microscopy (TEM) analysis by dispersing the catalyst powders in high-purity ethanol and allowing a drop of the suspension to dry on a carbon film supported on a 200-mesh Cu TEM grid. Bright-field (BF) imaging and selected-area ring diffraction patterns were acquired using a Philips CM12 operating at 200 keV with a W filament. Particle size histograms were calculated from sets of 200 particles.

2.3.5 Temperature programmed reduction

Temperature programmed reduction (TPR) analysis was carried out on a Thermo TPD/R/O 1100 Series instrument equipped with a thermal conductivity detector (TCD). The sample (100 mg) was heated up to 800°C at a ramp rate of 5 °C min^{-1}, under a flow of hydrogen (10% in Ar, 20 mL min^{-1}). For activation energy determination, heating ramp rates of 10, 15 and 20°C min^{-1} were also used.

Calibration of the TPR plots for the Au^{3+} amount was carried out for the Au/C sample prepared at 140 ^{o}C and using HCl as a solvent used as standard.

2.3.6 Titration of carbon functional groups

Acidity of carbon functional groups was carried out using a potentiometric method with a pH-meter [28] in a manner complementary to the Boehm protocol [29] which uses bases of different strength followed by back titration with HCl. Typically, the sample to be analysed (100 mg) was suspended in deionised water (10 mL) with stirring, and dilute HCl (0.02 M) or NaOH as appropriate, added step-wise (200 μL) and the pH measured after a stabilisation time (typically 1 minute) after each addition. Quantification of the functional groups was carried out by plotting the pH against volume of titrant added, and pK_a values of the carbon functional groups were identified.

3. Results and discussion

3.1 Effect of the impregnation drying temperature on the catalyst activity

The activity of the Au/C catalyst prepared *via* impregnation using *aqua regia* and a drying temperature of 110 ^{o}C is reported in Fig. 1. It is possible to observe that the catalyst initially exhibit low conversion (*ca.* 15%) followed by an increase in activity after about 3 h per time on stream, up to eventually reach *ca.* 50% conversion after 5 h. It should be highlighted that for all the tests carried out and reported in the current study the selectivity to VCM was virtually 100% with traces amounts (< 0.1%) of 1,2-dichlorethane and chlorinated oligomers only [9, 10, 12].

Previous studies on Au/C catalysts for hydrochlorination [10, 11] showed a monotonic deactivation trend ascribed to the reduction of Au^{3+} to Au^{0} and not an activity trend with enhanced activity per time on stream. On the other hand, for the catalyst reported in the present study, XRPD patterns permit an estimate of a mean particle below 4 nm, while in previous cases catalysts having an average particles size > 5nm were used, and this could affect the observed trend. As differences in drying

temperature could also affect the different particle size and the interface metal/support, two catalysts were prepared using a drying temperature of 140 and 180 ^{o}C (Fig. 1 and Fig. S1). The temperature of 180 ^{o}C was chosen because equals to the reaction temperature. This could possibly provide indications if the conversion trend could be affected by the drying temperature, if the catalysts were dried below 180 ^{o}C. However, it is also possible that these discrepancies with previous studies are also due to a sintering of the Au nanoparticles after reaction with the particular kind of carbon used, although this effect was not observed when *aqua regia* was used as a solvent (see paragraph 3.5). The catalyst dried at 185 ^{o}C has a similar trend to those dried at 110 ^{o}C, in contrast, the one dried at 140 ^{o}C is markedly different with an increase in activity from *ca*. 10% at the beginning of the reaction up to 70% after 5 h of time on stream. In order to assess if the catalyst reached steady state condition with a maximum of activity after 5h, a 12h catalytic test was carried out (Fig. S2). It was possible to observe that after 5h the steady state performance had been obtained.

3.2 *Aqua regia* as a solvent and contribution of HCl and HNO_3 to the catalyst activity

Investigation on the activity of *aqua regia* and studies on its activity have been so far limited to dissolution and corrosion studies with limited applications in the area or organic synthesis as chlorinating agent [30, 31]. In contrast, the use of solely HNO_3 with carbon matrixes has been the subject of investigations as HNO_3 can increase the number of oxygenated groups at the carbon surface. While HCl, despite a limited effect to carbon surfaces, can affect the nucleation process of metal nanoparticles, especially gold, from the metal salt precursors [32]. It should be noted that, in case of Au/C catalysts, once gold was deposited on the carbon surface, subsequent treatments with *aqua regia* were not capable of dissolving the gold, but rather change its oxidation state re-oxidizing it [13].

In view of this, and to investigate the effects of these two acids, catalysts obtained by impregnating the Au precursor from solutions containing only concentrated nitric acid (Fig. 2 and Fig. S3) and hydrochloric acid (Fig. 3 and Fig. S4) were used. Also in this

case, the effect of different drying temperatures was evaluated using 110, 140 and 180 ^{o}C. Considering the whole set of catalysts, the most active was the material prepared in *aqua regia* dried at 140 ^{o}C, with an activity of >70% to VCM after 5 h time on stream. However, for drying temperatures of 110 and 185 ^{o}C the most active catalyst was the one obtained using HNO_3 only as a solvent, with conversion values in the range of 60 and 70%. In contrast, the materials prepared using HCl only, always displayed lower activity, in the range of 20-30%. This is an important experimental result because it can shed light on the role that HNO_3 and HCl play on the final catalyst activity and stability of the catalyst. The enhanced effect of HNO_3 could be ascribed to enriched Au^{3+} content or modifications to the carbon surface structure [33, 34]. On the other hand it should be considered that Cl^- anions are well known nucleation centres for Au clusters and promoting sintering [32, 35]. This is well evident from the XRPD patterns of catalysts dried at 140 ^{o}C (Fig. 4) using HCl, HNO_3 and *aqua regia* as solvent. The sample obtained using HCl contains large Au particles, estimated in the range from 30 to 50 nm, while in those prepared using *aqua regia* or HNO_3, the particles size was estimated in the range of 20 nm. In addition, the XRPD patterns highlight that the drying temperature has an effect on the nucleation process of Au particles. In fact, using a temperature of 110 ^{o}C no discernible Au reflection is detected, indicating particles below 4 nm or a material with a large amount of Au^{3+} centres. Finally, the Au reflection intensity in case of HCl progressively increase (and so Au reduction) as long as the drying temperature is increased.

3.3 Modification induced to the catalyst structure by HCl, HNO_3 and *aqua regia* at different drying temperatures

Since previous literature studies ascribed the activity of the catalyst to the presence of Au^{3+} species postulating them as active sites [9-11, 13] XPS was systematically carried out for the samples dried at the three different temperatures in presence of HCl, HNO_3 and *aqua regia* (Fig. 5, Table 1 and Table 2) in order to quantify surface Au^{3+}. It is immediately evident that the material prepared at 110 ^{o}C presents a high amount of Au^{3+}, which was estimated between 43 and 67% (Table 1). As the drying temperature is increased, the amount of Au^0 increased, and this can relate with the reduction property of carbon towards Au^{3+} [11, 36]. However, considering both the XPS signal intensity (Fig. 5) and the intensity of the Au reflections detected by XRPD

(Fig. 4), a counter-intuitive obervation is obtained. From the XPS data, the samples prepared using HCl have invariably a higher intensity. Because XPS is a surface technique the signal is a function of the surface to bulk atoms ratio, therefore this trend would be explained by a decrease in the Au particle size. However, this is exactly the opposite trend obtained by XRPD, which is a bulk technique, where larger particles would lead to a higher signal. On the other hand there is another important aspect that needs to be considered, *i.e.* HNO_3 is known to induce textural changes in carbon [18, 34, 37] by changing the pore size, as well as functional groups on the surface, while HCl basically does not. In view of this, the different intensity of Au signal from XPS would arise by the presence of Au at different depths in the carbon support. It is extremely interesting to note (Table 3) that a quantification of the atomic species present on the catalysts surface shows a systematic, decreasing trend, of the Au/C surface ratio with the sequence HCl > HNO_3 > *aqua regia*, regardless the drying temperature used. And this trend is exactly the one that would be expected for the oxidizing force of the acids used, and therefore capable to alter the support properties.

In view of this, because all the catalysts were prepared *via* impregnation at the same gold loading, to match the trend observed using XPS and XRPD, the decreasing in Au/C surface ratio could be explained assuming that when HNO_3 is present, gold particles are present also inside the carbon pores and not just at the surface of it. To test this hypothesis all the samples were characterized by means of SEM-EDX (Table 3). Unlike XPS, which is a pure surface technique, (and that for our purposes it can be considered capable of a penetration depth of *ca.* two monolayers), SEM-EDX is a technique capable to penetrate the samples for few microns, and therefore capable to detect sub-surface particles. SEM-EDX proved to be more sensitive to the local composition of the samples, which were found to have a highly non homogenous composition distribution (see supplementary data, Figs. S5 to S14). In fact, while the XPS samples were prepared using ground samples, for the SEM-EDX analysis extrudates were directly analyzed in order to ensure flat surfaces to analyze. Also in this case, a decreasing surface gold content was detected, in addition it was possible to systematically highlight that, as long as HNO_3 was present a strong oxidation of the carbon support was detected, and thus corroborating the results obtained *via* XRPD and XPS. It should also be noted that SEM-EDX, unlike XPS detected the presence of additional elements (Al and S) (Table 3) This is observed for the following reasons:

the analysed area in EDX is 1 x 1 mm, while in the XPS is 0.3x0.4 mm, therefore cable of intrinsically detect elements in low amount with a lower detection limit. In addition, SEM-EDX is substantially a bulk technique when compared with XPS, which is purely surface sensitive, and the EDX penetration depth through the carbon extrudes we analyzed is almost 100%, thus sampling almost the entirely of the bulk in the analysed area, under the cross section of the SEM beam. Therefore atomic percentages such as 0.03% Al for example is at/beyond the limits of the XPS detection and so with such percentages any at the surface would be undetectable.

TEM was also carried out (Table 4, Figs. S15 - S23), showing that the samples dried at 110 ^{o}C, had a particle size in the range of 3 nm, while for the samples dried at 140 ^{o}C, the particle size order per solvent was: HCl >HNO_3 ≈, *aqua regia* ranging from *ca*. 66 to 20 nm, and finally for the samples dried at 180 ^{o}C the particle size order per solvent was HCl > HNO_3 >*aqua regia*, ranging from *ca*. 67 to 3 nm These values are broadly similar to those obtained by XRPD, due to lack of homogeneity of the distribution of the gold nanoparticles both on the surface and within the pores of the carbon support. In fact, it was possible to identify some catalyst regions are rich in metal nanoparticles, while in others the particles are nearly absent (see supplementary data, Fig. S24). This inhomogeneity could be due to intrinsic properties of the wetness impregnation technique used in this case. Similar phenomena have been reported for impregnated solutions of platinum salts on carbon [38] after thermal treatment for impregnation. This is also reflected in the wide particle size distribution obtained *via* TEM (Table 4, and Figs S15 to S23). In fact the particles size values obtained *via* XRPD are invariably lower than those obtained using TEM, because of this wide distribution that further contribute to the line broadening of the XRD peaks [39,40].

3.4 Effect of HCl:HNO_3 ratio and TPR analysis of Au/C catalysts

The results reported so far, shed light also in a further important aspect of this reaction; at present all the studies on the reaction mechanism reported for this reaction postulated Au^{3+} associated with Au nanoparticles as active sites, and a strong dependency of the activity on the [Au^{3+}] [7-13]. On the other hand it is quite clear, from the data reported above, that the catalysts with very high Au^{3+} content (> 50%, for the materials dried at 110 ^{o}C), are not the most active. In addition, while it is

confirmed the effect of HNO_3 on the final catalyst by enhancing its activity, no obvious difference is present for the samples treated with HNO_3 when different drying temperatures are used. It should be stressed that all the current models explaining the activity of the Au/C catalysts, proposed the existence of Au^{3+} at the surface of Au nanoparticles, while the data collected show that it is possible that the activity also relates with the presence of active sites at the interface Au/C, and therefore below the detection limit of the characterization methods currently available.

It should also be considered that the final activity could be due to changes in Au^{3+} concentration, (as well as particles sizes) and it is also known that the activity can be a complex function of the feed composition and reaction conditions. In fact, it was previously observed [10] that an excess of HCl in the feed can promote the reaction, while an excess of C_2H_2 has a detrimental effect. In view of this, and to systematically evaluate the effect of HNO_3, a set of nine catalysts were prepared with different HCl:HNO_3 ratio with a HNO_3 volume fraction spanning from 0 to 1 (Fig. 6 and Fig. S24) and these were evaluated for acetylene hydrochlorination. It is observed that the most active catalyst (> 70% conversion) is that prepared using the 0.25 HNO_3 volume fraction, *i.e.* the *aqua regia* composition, but also in this case no apparent trend is present when the HNO_3 composition was changed from this optimal value. This led us to expand our investigation by focusing on changes that the acids can induce on the carbon support rather than Au nanoparticles only, and the effect that these acids can have on the interaction metal/support and in turn to the Au/C interface.

Activated carbon is not a matrix constituted by carbon only as element, but it is has a complex structure characterized by the presence of oxygen in form of carboxylic, ester, ether and lactone groups [18, 41] as well as heteroatoms e.g. phosphorus nitrogen or sulphur, present as phosphates, amine and thiols [42]. In order to identify the variation of the materials prepared using *aqua regia*, and to ascertain the importance of Au^{3+} centres in the catalyst performance, and the effects that these acids can have on the carbon matrix, the catalysts described so far were evaluated by means of TPR focusing on the samples prepared at 140 ^{o}C, which appears to be the temperature capable to lead to the most active materials.

A representative example of TPR profiles of catalysts prepared in HCl, HNO_3 and *aqua regia* dried at 140 °C, as well as carbon support, is shown in Fig. 7. The

analysis of this thermogram led to assign the reduction band between 230 and 300 ^{o}C to Au^{3+} [43], while those from 450 to 800 ^{o}C are the consequence of decarboxylation reactions of oxygenated carbon functional groups at the carbon surface, which release CO and CO_2. Particularly, decarboxylation reactions in the range of 400-650 ^{o}C are ascribed to carboxylic acids and carboxylic anhydrides [44], while above 650 ^{o}C these are likely due to lactones and phenols [45].

It is interesting to note (Fig. 7) how the areas of the reduction peaks observed for the catalysts in the range 350-650 ^{o}C, *i.e.* for signal originating from carbon oxygenated groups, follow the trend HNO_3 > *aqua regia* > HCl, and this would be consistent with the oxidizing effect of these acids. In fact as HNO_3 has the greater oxidizing effect it is also expected to increase the amount of oxygen containing functional groups over the carbon surface [18, 44] and the different features observed for different acids could be associated to the generation of new functional groups, either on the carbon surface or at the carbon/gold interface. This is an aspect that at present has been ascertained for Pt/C based catalysts, where investigations on the chemistry of the impregnation of hexachloroplatinic acid on carbon as support, leads to conclude the presence of Pt in two different oxidation states as the consequence of two different ligand carbon sites [38]. One type consisting of oxygen-containing functional groups on the basal plane edges, and the other consisting of π-complex structures in the carbon basal plane [46,47]. It is likely that similar phenomena could occur during gold impregnation as well. In addition, studies on the effect of acids on carbon, showed that while HNO_3 has an oxidative effect, in the case of HCl, Cl^- can bind to sp^2 carbon sites on the carbon matrix [48]. In our case, this could act as an inhibitor for nucleation centres for active metals on basal planes, and could explain the lack of activity of materials prepared containing HCl only, and thus indirectly suggesting the binding sites of gold to carbon.

Therefore, in order to identify features that could be due to the effect of the acid on the support, or by the simultaneous presence of Au clusters, the carbon support was treated in an identical manner to that of the catalyst preparation but without adding of $HAuCl_4$. When gold was not present (Fig. 8) the thermograms showed, as expected, features between 350 and 650 ^{o}C only, and these should be considered as originated

just from the support. However, the thermal profiles are different when compared to the materials containing gold, because in its absence a lower number of reduction (decarboxylation) peaks are detected. This is an important aspect, because it would suggest the presence of an interface Au/C, mediated by oxidized carbon groups, that affects the carbon surface.

In view of this, TPR analysis was carried out on the samples prepared using all the HCl:HNO_3 mixtures, and the signal integration of the Au^{3+} species versus HNO_3 volume fraction is reported in Fig. 9. A volcano plot with maximum centred between 0.5 and 0.6 HNO_3 volume fraction is obtained. However, despite being these the catalysts with the highest amount of Au^{3+}, they are not the most active, but the material prepared *aqua regia* with a HNO_3 fraction of 0.25. This result, would suggest that the most active catalyst is not necessarily the material with the highest Au^{3+} content, but possibly the material that has Au^{3+} at the appropriate catalyst sites. It should also be noted that the Au^{3+} (%) amounts obtained by TPR are higher (of *ca.* 20% relative amount) than those obtained using XPS, thus confirming the presence of Au atoms/clusters below the carbon surface because of modifications induced by HNO_3. The data collected so far, would suggest the existence of sites at the interface Au/C and not just at the surface of Au nanoparticles.

A further, important aspect, to consider in this analysis, is the reduction temperature of the various catalysts under TPR conditions. From Fig. 10 it appears immediately evident that the *aqua regia* catalyst, is the one with the lowest Au reduction temperature (258 ^{o}C), thus showing that not only the presence of Au^{3+} is important, but also the reducibility of this species is determining the final activity.

In view of this, we were interested to determine the effect that an acid treatment on the carbon support, before gold deposition could have had on the final catalytic performance. Acid pre-treatment is not unprecedented, and so far it found important applications in the direct synthesis of H_2O_2 over gold catalysts [49, 50] or CO oxidation over Pd -based catalysts [18]. In our case, when the support was pre-treated with HCl, HNO_3 or *aqua regia*, the final catalysts were invariably less active than the catalysts obtained when the gold precursor was present simultaneously with the acid during the impregnation step. This shows that although different acids do have a

significant effect on the carbon surface, in terms of the functional groups present, it seems more important how the gold interacts with these functional groups at the surface of the carbon support at the time of the deposition. This is an area that so far received limited attention and this is most likely due to the difficulties of investigating the deposition process of metals on carbon supports, and at present virtually no studies are available concerning Au deposition. It is generally assumed that functional groups on the carbon surface can act as anchoring sites for metal complexes. As no studies are present for $HAuCl_4$, it could worth considering the case of H_2PdCl_4 as Pd(II) is isoelectronic with Au(III) and the $[PdCl_4]^{2-}$ anion is square planar as is $[AuCl_4]^-$. In the case of H_2PdCl_4 the binding process on carbon is considered to proceed *via* interaction with olefinic π-fragments over the carbon surface by exchange of Cl ligands [51]. On the other hand, the $[PdCl_4]^{2-}$ anion can bond *via* ion exchange over protonated oxygen containing groups [18]. It is considered likely the same process takes place in case of $HAuCl_4$.

3.5 Base titration of carbon and Au/C catalysts and characterization on the catalysts after reaction

To further test this assumption, *i.e.* the dominant role of oxygenated groups at the interface of Au/C, titrations of the acid pre-treated carbons and Au/C catalysts impregnated using HCl, HNO_3 and *aqua regia*, were carried out using NaOH as the titrating agent.

For the pre-treated carbons, it is possible to observe a correlation between the amount of HNO_3 used in the preparation and the number of carboxylic/lactones groups generated by the treatment. In fact while HCl has an almost negligible effect, *aqua regia* increases the number of oxygenated functionalities observed on the carbon surface, and HNO_3 can further increase this with a ratio of *ca.* 2.5 times (Fig. 11). Thus showing that HNO_3 can modify the carbon support and in turn the catalytic activity, and we consider this effect is most likely caused by modifying the anchoring of Au^{3+} precursor to the support. The titrations carried out on the Au/C catalysts from acid pre-treated carbons are very similar to those on the final catalysts within experimental error, thus supporting the hypothesis that if changes between the carbon

and the catalyst has to be present at the Au/C interface and the exposed carbon surface remains basically unmodified in terms of amount and kind of functional groups.

As the carbon surface can affect the Au carbon interface, and in turn the possible particles agglomeration under reaction conditions, all the catalyst prepared using HCl, HNO_3 and *aqua regia* prepared at the drying temperatures of 110, 140 and 180 ^oC were analysed after reaction *via* XRPD in order to estimate if any sintering was present (table 4 and Fig. S25) Sintering was observed for the catalyst prepared using HCl and HNO_3 as a solvent, but not for the catalysts prepared using *aqua regia*, independently from the initial drying temperature of the catalyst. A similar effect for a catalyst prepared in *aqua regia* was observed for Au/C catalyst as determined by TEM [10] although using a different kind of carbon.
While the sintering effect could explain the differences in activity trend per time on-stream for the catalysts prepared using HCl and HNO_3, as this does not happen for the catalysts using *aqua regia*, the catalyst behaviour could be affected by modification of species at the Au/C interface. Another factor could be the reduction of Au^{3+} centres during the reaction, as ascertained by previous studies [11-13].

3.6 Kissinger equation and compensation plot

Additional information can be extracted from TPR analysis, by varying the ramp rate of the heating [52]. In this case, assuming an Arrhenius dependence of the rate constant of the reduction reaction, and knowing the reaction order model, it is possible to determine the activation energy of a reduction reaction using the Kissinger equation [53, 54].

$$\ln (\beta/T^2_{max}) = \ln (AR/E_a) + \ln [n(1-\alpha_{max})^{n-1}] - E_a/RT_{max} \qquad \text{(eq. 1)}$$

Where E_a is the activation energy, A the pre-exponential factor, β the heating rate, n is the order of the reaction, α is the conversion degree, T is the temperature and R is the gas constant; the index *max* indicates the maximum of the reaction rate, with T_{max} the temperature at which the maximum of the Au^{3+} reduction step occurs. The equation

originally made use of differential thermal gravimetry, thermal analysis, or differential scanning calorimetry data and it has found application in the analysis of crystallization processes [55] or glass transition temperatures [56], because it has the advantage to rely on non-isothermal data. Reduction of Au^{3+} in lignite carbon matrixes, showed that the Au^{3+} to Au^{0} reduction occur *via* a first order kinetic [36]. Assuming in our case, the same kinetics, the equation 1 can be rewritten as:

$$\ln (\beta/T^2_{max}) = \ln (AR/E_a) - E_a/RT_{max} \quad \text{(eq. 2)}$$

It is then possible to determine the activation energy of the reduction process and the pre-exponential factor, by plotting $\ln(\beta/T^2_{max})$ versus 1/T from the slope and the intercept of the resulting straight line respectively.

TPR profiles were collected using temperature ramps of 5, 10 and 15 ^{o}C for the catalysts prepared in HCl, *aqua regia* and HNO_3 , dried at 110, 140 and 185°C (see supplementary data, Figs S26 to S34). The values obtained for the activation energies are shown in table 5. The activation energies, were in a range from 40 kJ mol^{-1} for the catalyst prepared using *aqua regia* to 70 kJ mol^{-1} for the catalyst obtained *using* HCl (both dried at 185 ^{o}C). Interestingly, the most active catalyst for the hydrochlorination reaction of acetylene, *i.e.* the material obtained using *aqua regia* impregnated at 140 ^{o}C with an intermediate activation energy for the Au^{3+} reduction of *ca.* 50 kJ mol^{-1}.

Considering the effect of the reducibility of Au^{3+} so far observed in the activity for the hydrochlorination reaction, *i.e.* the more reducible a catalyst the more active it is, the expected trend would have been that: the higher was the E_a for the reduction of Au^{3+} and the lower to be the conversion for the hydrochlorination reaction. However, when the conversion of the hydrochlorination reaction was plotted versus the E_a for the Au^{3+} reduction, a decrease in activity of the catalysts at lower activation energies is detected (Fig. 12 and Fig. S35) with a maximum at *ca.* 50 kJ/mol. This suggests that there may be a threshold, below which the gold is too reducible to be active, *i.e.* it will completely reduce, (and possibly sinter), rather than be involved in a redox cycle, which is one of the postulated mechanism of action for this material [9-11]. On the other hand we should also consider that the experimental error associated with the

activation energy is relatively high, ranging from *ca.* 7 to 12%, therefore this correlation does not pretend to be a strict mathematical model. Though, it can be an alternative way to evaluate these catalysts, as the role of the reducibility of the metal centre is a factor so far neglected in many reactions involving gold. By comparison, literature values for the reduction (*i.e.* nucleation and growth) of Au^{3+} over supports like: SiO_2, MgO and TiO_2 span from 12 to 6 kJ mol^{-1} [55-57]. To date, none of the Au catalysts prepared using supports other than carbon [7-12] has been found to be active for the hydrochlorination reaction of acetylene, and this confirms that carbon can stabilize Au^{3+} species. On the other hand, it is important to underline that we are attempting to extract information from a reduction process by means of using H_2 as a probe when the hydrochlorination reaction is likely to occur *via* formation of a C_2H_2/Au/HCl complex where a simultaneous approach of the two substrates take place over Au^{3+} centres [9, 10], and hence this can induce limitations in our model. Nevertheless, it is still possible to correlate the ln*A* to the E_a of the reduction process in a compensation plot (Fig. 13). Since a straight line is obtained this indicates an Arrhenius dependence of the rate of the Au^{3+} reduction on temperature, and that there is a common factor linking the number of collisions with the activation energy of the catalyst and this factor is likely to be the amount of Au^{3+} centres.

4. Conclusions

Aqua regia was found to prepare the most efficient catalysts for the hydrochorination of acetylene by impregnation of $HAuCl_4$ on carbon. The effect of the *aqua regia* constituents, HCl and HNO_3, was also evaluated, and despite these acids being able to affect the carbon support prior deposition, the enhancement effect observed with *aqua regia* occurs only in case of simultaneous presence of Au during the impregnation step of the catalyst preparation. This is considered to be due to a combination of the oxidising effect of HNO_3 on the carbon support and gold, as well as a nucleation effect of HCl to gold particles over the carbon surface and the two acids are then capable to act synergistically. Interestingly, it was also noted that when *aqua regia* was used as a solvent no detectable sintering was observed after reaction.

It has also been shown that TPR is a useful characterisation technique for Au^{3+} species in Au/C catalysts, since it is able to provide information on the Au species and the carbon support as well as to the determination of kinetic parameters for the reduction of Au^{3+}. Many factors have been found to contribute to the final activity of these catalysts, like the particles size, modification of the carbon support functional group, as well as the amount of Au^{3+}, with effects difficult to predict *a priori*. On the other hand this study showed that the efficiency of the catalyst could not only depend on the amount of Au^{3+} as previously postulated [9-11], but it could also be due to the easiness of reducibility of these oxidised gold species. In turn, this is likely to be related with the location of Au^{3+} not just at the surface of the catalyst, but also that the interface Au/C, and this is an important aspect so far neglected for this class of catalyst for this kind of reaction.

Acknowledgements The authors thank Johnson Matthey Plc and World Gold Council for financial support.

References

[1] K. Weissermel, H.-J. Arpe, *Industrial Organic Chemistry* (4th edition), Wiley-VCH, Weinheim, 2003, p 217.

[2] J.G. Speight, *Chemical and Process Design Handbook*, McGraw-Hill, New York, 2002, p 2.542.

[3] I.M. Clegg, R. Hardman, US Patent 5763710, 1998.

[4] K. Shinoda, Chem. Lett. 4 (1975) 219-220.

[5] S. Matar, L.F. Hatch, *Chemistry of chemical processes* (2nd edition), Butterworth-Heinemann, Woburn, Massachusetts, 2001, p 202.

[6] United States Environmental Protection Agency, Entry file EPA/600/X-84/178, Washington D.C., 1988.

[7] G.J. Hutchings, J. Catal. 96 (1985) 292-295.

[8] B. Nkosi, N.J. Coville, G.J. Hutchings, J. Chem. Soc., Chem. Comm. (1988) 71-72.

[9] G.J. Hutchings, Gold. Bull. 29 (1996) 123-130.

[10] M. Conte, A. F. Carley, C. Heirene, D.J. Willock, P. Johnston, A,A. Herzing, C.J. Kiely, G.J. Hutchings, J. Catal. 250 (2007) 231-239.

[11] B. Nkosi, N.J. Coville, G.J. Hutchings, M.D. Adams, J. Friedl, F.E. Wagner, J. Catal. 128 (1991) 366-377.

[12] B. Nkosi, M.D. Adams, N.J. Coville, G.J. Hutchings, J. Catal. 128 (1991) 378-386.

[13] M. Conte, A.F. Carley, G.J. Hutchings, Catal. Lett. 124 (2008) 165-167.

[14] A.S.K. Hashmi, G.J. Hutchings, Angew. Chem., Int. Ed. 45 (2006) 7896-7936.

[15] A. Arcadi, Chem. Rev. 108 (2008) 3266-3325.

[16] G.J. Hutchings, Chem. Commun. (2008) 1148-1164.

[17] A. Corma, H. Garcia, Chem. Soc. Rev. 37 (2008) 2096-2126.

[18] M. Gurrath, T. Kuretzky, H.P. Boehm, L.B. Okhlopkova, A.S. Lisitsyn, V.A. Likholobov, Carbon 38 (2000) 1241-1255.

[19] M.A. Fraga, M.J. Mendes, E. Jordão, J. Mol. Catal A: Chem. 179 (2002) 243-251.

[20] A. Corma, A. Leyva-Pérez, M. J. Sabater, Chem. Rev. 111 (2011) 1657-1712.

[21] A. Villa, G.M. Veith, L. Prati, Angew. Chem., Int. Ed. 49 (2010) 4499-4502.

[22] T. Mallat, A. Baiker, Chem. Rev. 104 (2004) 3037-3058.

[23] M.D. Hughes, Y.-J. Xu, P. Jenkins, P. McMorn, P. Landon, D.I. Enache, A.F. Carley, G.A. Attard, G.J. Hutchings, F. King, E.H. Stitt, P. Johnston, K. Griffin, C.J. Kiely, Nature 437 (2005) 1132-1135.

[24] T.A. Nijhuis, T. Q. Gardner, B. M. Weckhuysen, J. Catal. 236 (2005) 153-163.

[25] A. Wittstock, V. Zielasek, J. Biener, C. M. Friend, M. Bäumer, Science 327 (2010) 319-322.

[26] B.D. Cullity, S.R. Stock, *Elements of X-Ray Diffraction*, (3rd edition), Prentice-Hall Inc, Upper Saddle River, 2001. p161

[27] J.I. Langford, J. Appl. Cryst. 11 (1978) 10-14.

[28] A. Contescu, C. Contescu, K. Putyera and J.A. Schwarz, Carbon , 35 (1997) 83-94.

[29] H.P. Boehm, E. Diehl, W. Heck, R. Sappok, Angew. Chemie 76 (1964) 742-751.

[30] R.G. Raptis, J.P. Fackler Jr., Inorg. Chem. 29 (1990) 5003-5006.

[31] M. Calleja, K. Johnson, W.J. Belcher, J.W. Steed, Inorg. Chem. 40 (2001) 4978-4985.

[32] H.-S. Oh, J.H. Yang, C.K. Costello, Y.M. Wang, S.R. Bare, H.H. Kung, M.C. Kung, J. Catal. 210 (2002) 375-386.

[33] E.G. Rodrigues, M.F.R. Pereira, X. Chen, J.J. Delgado, J.J.M. Órfão, J. Catal. 281 (2011) 119-127.

[34] H. Tamon, M. Okazaki, Carbon 34 (1996) 741-746.

[35] B.S. Uphade, M. Okumura, S. Tsubota, M. Haurta, Appl. Catal. A: Gen. 190, (2000) 43-50.

[36] J.-P. Gatellier, J.-R. Disnar, Org. Geochem. 16 (1990) 631-640.

[37] N. Zhang, L.-Y. Wang, H. Liu, Q.-K. Cai, Surf. Interface Anal. 40 (2008) 1190-1194.

[38] M. Kang, Y.-S. Bae, C.-H. Lee, Carbon, 43 (2005) 1512-1516.

[39] J. Gubicza, J. Szépvölgyi, I. Mohai, L. Zsoldos, T. Ungár, Mat. Sci. Eng. A, 280 (2000) 263-269.

[40] Y.Dieckmann, H.Cölfen, H. Hofmann, A. Petri-Fink, Anal. Chem. 81 (2009) 3889-3895.

[41] C. Moreno-Castilla, M.A. Ferro-Garcia, J.P. Joly, I. Bautista-Toledo, F. Carrasco-Marin, J. Rivera-Utrilla, Langmuir 11 (1996) 4386-4392.

[42] J.K. Brennan, T.J. Bandosz, K.T. Thomson, K.E. Gubbins, Colloids and Surfaces A: Physicochem. Eng. Aspects 187-188 (2001) 539-568.

[43] C. Baatz, N. Decker, U. Prüße Journal of Catalysis 258 (2008) 165-169.
[44] S.R. de Miguel, O.A. Scelza, M.C. Román-Martínez, C. Salinas-Martínez de Lecea, D. Cazorla-Amorós, A. Linares-Solano, Appl. Catal. A: Gen. 170 (1998) 93-103
[45] J.L. Figueiredo, M.F.R. Pereira, M.M.A. Freitas, J.J.M. Órfão, Carbon 37 (1999) 1379-1389.
[46] F. Coloma, A. Sepulveda-Escribano, J.L.G. Fierro, F. Rodriguez-Reinoso, Langmuir 10 (1994) 750-755.
[47] D.E. van Dam and H. van Bekkum, J. Catal. 131 (1991) 335-349.
[48] E. Papirer, R. Lacroix, J.-B. Donnet, G. Nansé, P. Fioux, Carbon 33 (1995) 63-72.
[49] E.N. Ntainjua, M. Piccinini, S.J. Freakley, J.C. Pritchard, J.K. Edwards, A.F. Carley, G.J. Hutchings, Green Chem. 14 (2012) 170-181.
[50] J.K. Edwards, B. Solsona, E.N. Ntainjua, A.F. Carley, A.A.Herzing, C.J. Kiely, G.J. Hutchings, Science 323 (2009) 1037-1041.
[51] P.A. Simonov, A.V. Romanenko, I.P Prosvirin, E.M. Moroz, A.I. Boronin, A.L. Chuvilin, V.A. Likholobov, Carbon 35 (1997) 73-82.
[52] G. O. Piloyan, I. D. Ryabchikov, O. S. Novikova, Nature 212 (1966) 1229.
[53] P. Budrugeac, E. Segal, J. Therm. Anal. Cal. 88 (2007) 703-707.
[54] H. E. Kissinger, Anal. Chem. 29 (1957) 1702-1706.
[55] L. Heireche, M. Belhadji, Chalcogenide Lett. 4 (2007) 23-33.
[56] N. Mehta, A. Kumar, J. Optoelectron. Adv. M. 7 (2005) 1473-1478.
Ea for nucleation energies
[57] K. Hojrup-Hansen, S. Ferrero, C.R. Henry, Appl. Surf. Sci. 226 (2004) 167-172.
[58] S.C. Parker, A.W. Grant, V.A. Bondzie, C.T. Campbell, Surf. Sci. 441 (1999) 10-20.

Tables, figures and captions

Table 1. Surface relative amount and binding energies of Au^{3+} and Au^{0} over Au/C catalyst prepared using HCl, HNO_3 and *aqua regia* dried at 110, 140 and 180 ^{o}C, determined by XPS.

Catalyst preparation		Au oxidation state		Binding energy	
Acid or mixture	Drying temperature (^{o}C)	Au^{3+} (%)	Au^{0} (%)	Au^{3+} (eV)	Au^{0} (eV)
HCl	110	67.3	32.7	86.8	84.2
HNO_3	110	43.6	56.4	86.8	84.8
Aqua regia	110	53.5	46.5	86.8	84.3
HCl	140	18.5	81.5	86.5	84.1
HNO_3	140	16.7	83.3	86.6	84.6
Aqua regia	140	22.3	77.7	86.5	84.1
HCl	180	12.4	87.6	86.3	84.2
HNO_3	180	18.9	81.1	86.3	84.1
Aqua regia	180	11.4	88.6	86.7	84.7

Table 2. Surface composition of Au/C catalyst prepared using HCl, HNO_3 and *aqua regia* dried at 110, 140 and 180 ^{o}C, determined by XPS.

Catalyst preparation		Elemental composition (%)						
Acid or mixture	Drying temperature (^{o}C)	Au 4f (%)	C 1s (%)	Cl 2p (%)	Na 1s (%)	O 1s (%)	Si 2p (%)	Au/C ratio (%)
HCl	110	0.10	95.63	0.56	0.00	3.29	0.43	0.100
HNO_3	110	0.06	87.11	0.23	0.00	12.01	0.59	0.072
Aqua regia	110	0.04	89.79	0.79	0.00	8.44	0.94	0.050
HCl	140	0.18	95.04	0.58	0.09	3.46	0.65	0.190
HNO_3	140	0.07	92.90	0.78	0.07	5.62	0.56	0.070
Aqua regia	140	0.03	90.37	0.20	0.00	8.80	0.60	0.033
HCl	180	0.10	95.79	0.30	0.07	3.19	0.55	0.106
HNO_3	180	0.08	92.75	0.88	0.00	5.76	0.53	0.081
Aqua regia	180	0.07	88.73	0.13	0.00	9.83	1.24	0.077

Table 3. Average composition of Au/C catalyst prepared using HCl, HNO_3 and *aqua regia* dried at 110, 140 and 180 ^{o}C, determined by SEM-EDX.

Catalyst preparation		Elemental composition (%)								
Acid or mixture	Drying temperature (^{o}C)	C	O	Na	Al	Si	S	Cl	K	Au
HCl	110	95.59	0.00	0.05	0.03	0.29	0.32	2.86	0.03	0.84
HNO_3	110	73.00	25.00	0.21	0.05	0.43	0.22	0.46	0.05	0.60
aqua regia	110	82.87	12.51	0.14	0.07	0.33	0.27	2.92	0.02	0.89
HCl	140	89.63	6.69	0.13	0.09	0.27	0.15	1.76	0.02	1.29
HNO_3	140	76.76	20.80	0.35	0.07	0.54	0.37	0.50	0.05	0.58
aqua regia	140	85.98	10.49	0.13	0.04	0.24	0.22	2.18	0.02	0.73
HCl	180	89.74	6.13	0.15	0.05	0.61	0.15	1.59	0.00	1.59
HNO_3	180	80.27	16.50	0.34	0.08	0.42	0.46	0.71	0.05	1.19
aqua regia	180	86.42	9.31	0.11	0.02	0.28	0.11	2.73	0.02	1.03

Table 4. Average Au particle size over Au/C catalysts prepared using HCl, HNO_3 and *aqua regia* dried at 110, 140 and 180 ^{o}C, determined by XRPD and TEM

Catalyst preparation		Au particle size		
Acid or mixture	Drying temperature (^{o}C)	Determination from XRPD ([a]). Fresh catalysts	Determination from TEM ([b]). Fresh catalysts.	Determination from XRPD ([a]). Spent catalysts.
HCl	110	< 4[c]	3 ± 2	28 ± 3
HNO_3	110	< 4[c]	3 ± 2	31 ± 3
aqua regia	110	< 4[c]	3 ± 2	< 4[c]
HCl	140	40 ± 10	66 ± 23	41 ± 10
HNO_3	140	20 ± 3	22 ± 4	20 ± 3
aqua regia	140	20 ± 3	22 ± 3	20 ± 3
HCl	180	40 ± 10	67 ± 23	42 ± 10
HNO_3	180	8 ± 1	9 ± 3	15 ± 2
aqua regia	180	< 4[c]	4 ± 2	< 4[c]

([a]) Error estimated from XRD peak broadening of 0.06 ^{o}at the Au (111) reflection at 38.18 ^{o} 2θ.

([b]) Error from particles size distribution from sets of 200 particles.

([c]) It was not possible to assign any error band below 4 nm, as this size is below the XRPD method.

Table 5. Activation energies for the reduction of Au^{3+} to Au^0 in presence of H_2 over Au/C catalysts.

Acid or mixture	Drying temperature (^oC)	E_a (kJ mol^{-1}) (*)
HCl	110	43.3 ± 5.3
HNO_3	110	43.0 ± 4.5
aqua regia	110	56.8 ± 5.5
HCl	140	53.6 ± 5.9
HNO_3	140	54.2 ± 2.6
aqua regia	140	50.4 ± 4.1
HCl	180	71.8 ± 5.0
HNO_3	180	45.0 ± 3.4
aqua regia	180	39.6 ± 2.6

(*) The experimental error for the activation energy, Ea, was calculated from the least square regression line of $\ln(\beta/T^2_{max})$ versus 1/T.

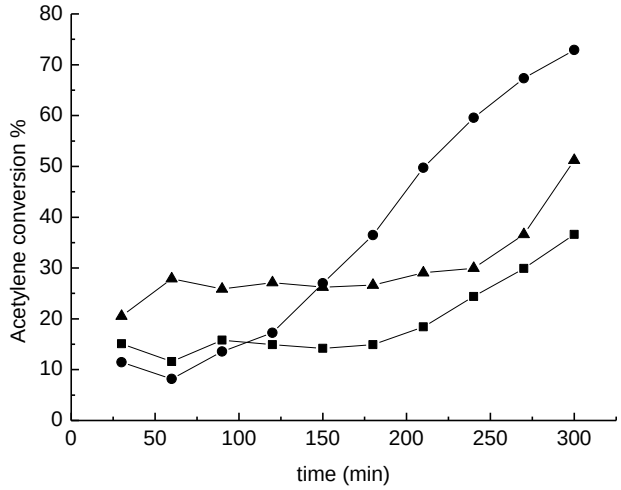

Fig. 1. Acetylene conversion by using catalysts impregnated in *aqua regia*, drying the catalysts at temperatures of: (■) 110, (●) 140 and (▲) 180 ^{o}C.

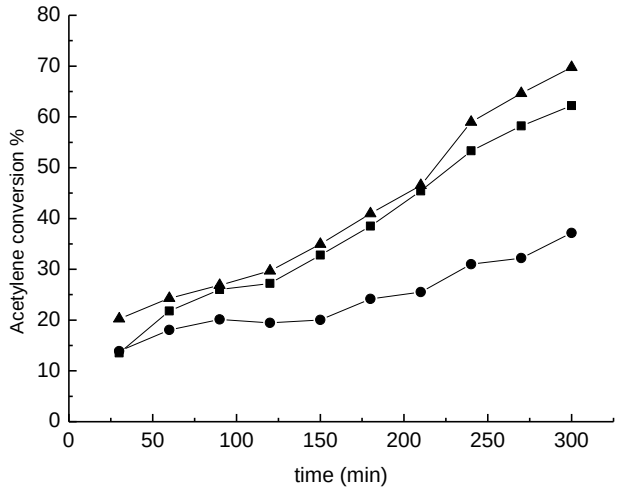

Fig. 2. Acetylene conversion by using catalysts impregnated in HNO_3, drying the catalysts at temperatures of: (■) 110, (●) 140 and (▲) 180 ^{o}C.

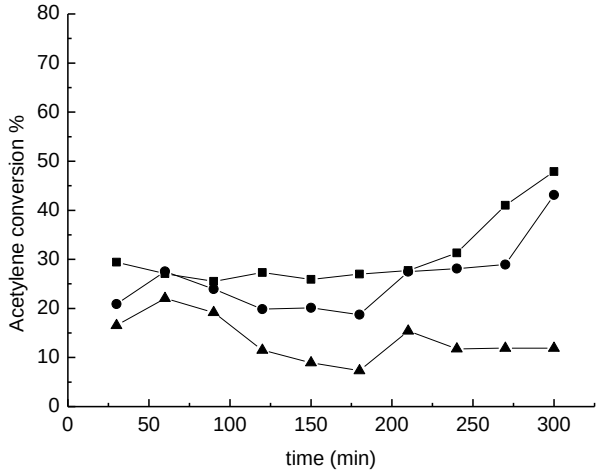

Fig. 3. Acetylene conversion by using catalysts impregnated in HCl drying the catalysts at different temperatures of: (■) 110, (●) 140 and (▲) 180 ^{o}C.

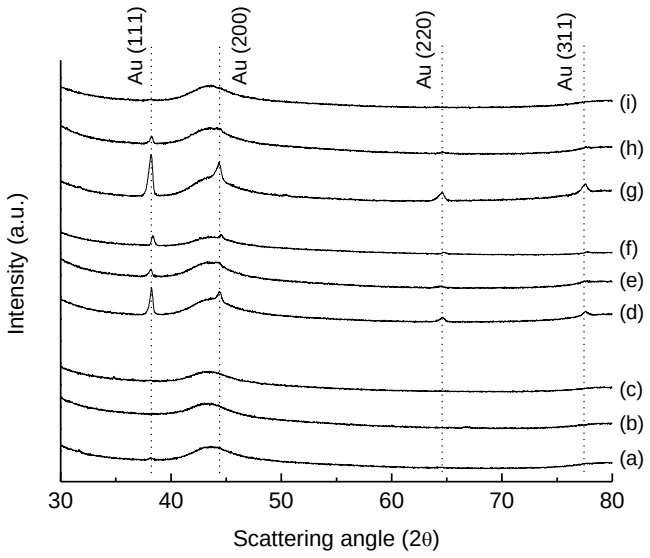

Figure 4. XRD patterns of Au/C carbon prepared accordingly to different solvent and drying temperature: (a) HCl, (b) HNO_3 and (c) *aqua regia* for catalysts dried at 110 ^{o}C; (d) HCl, (e) HNO_3 , and (f) *aqua regia* for catalysts dried at 140 ^{o}C; (g) HCl, (h) HNO_3 and (i) *aqua regia* for catalysts dried at 180 ^{o}C.

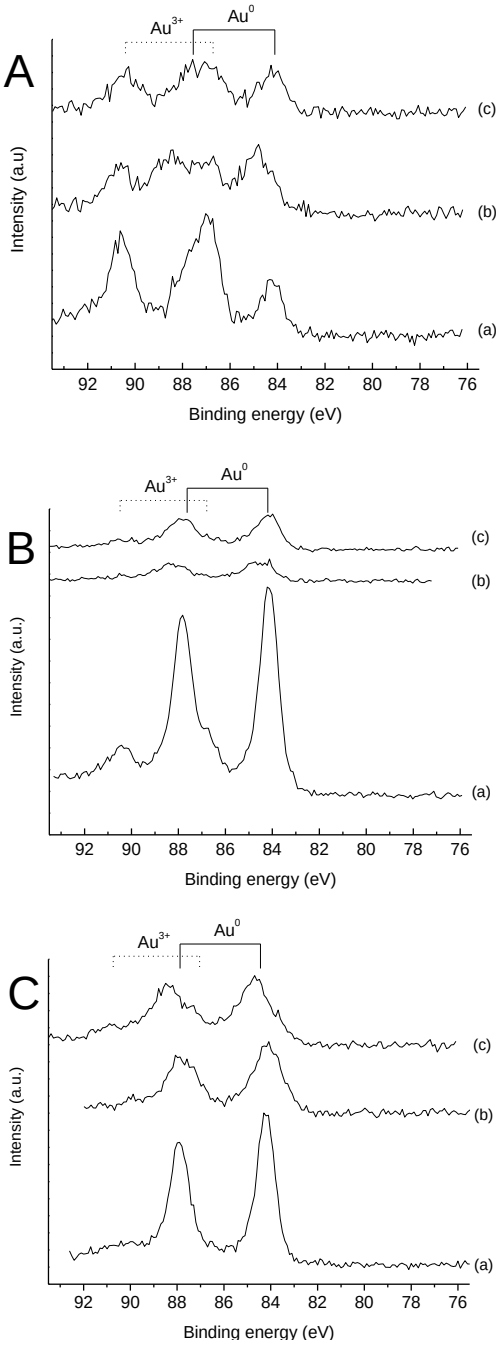

Figure 5. XPS spectra of Au/C carbon prepared accordingly to different solvent and drying temperature: A: (a) HCl, (b) HNO_3 and (c) *aqua regia* for catalysts dried at 110 ^oC; B: (a) HCl, (b) HNO_3 ,and (c) *aqua regia* for catalysts dried at 140 ^oC; C: (a) HCl, (b) HNO_3 and (c) *aqua regia* for catalysts dried at 180 ^oC.

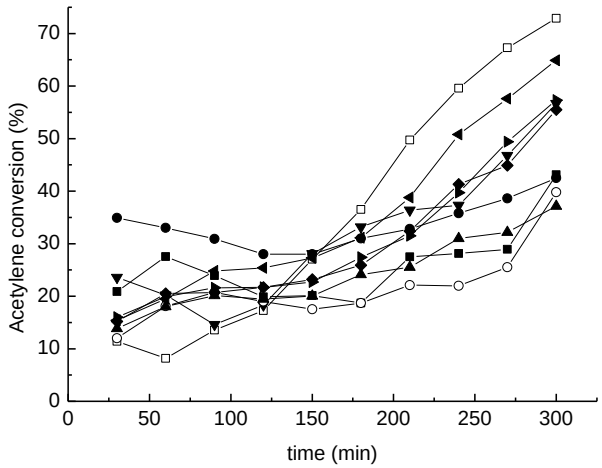

Figure 6. acetylene conversion over Au/C catalysts dried at 140 ^{o}C using different HNO_3 volume fraction in the HCl:HNO_3 preparation mixture: (■) 0, (●) 0.1, (□) 0.25, (▼) 0.33, (○) 0.5, (◄) 0.65, (►) 0.75, (♦) 0.9 and (▲) 1 HNO_3 volume fraction.

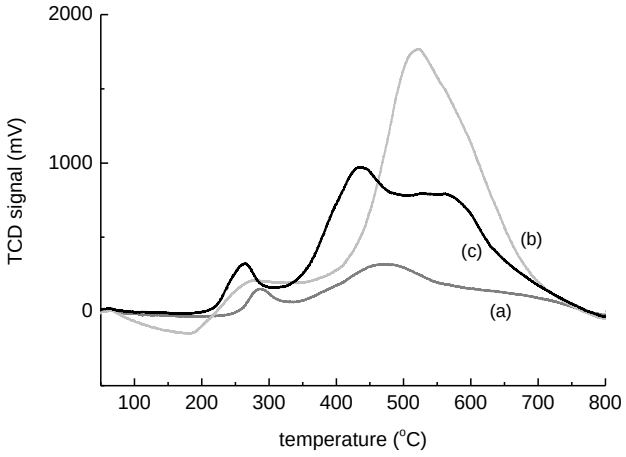

Figure 5. TPR profiles of Au/C catalysts dried at 140 ^{o}C prepared via impregnation using: (a) HCl, (b) HNO_3, and (c) *aqua regia* as solvent.

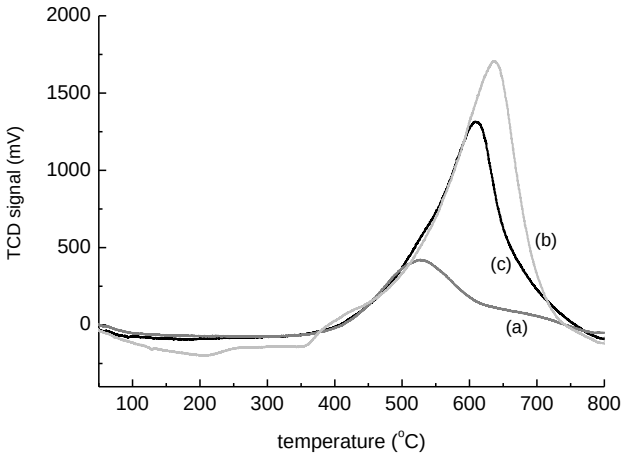

Figure 6. TPR profiles of carbon support Norit ROX 0.8 dried at 140 °C prepared via impregnation using: (a) HCl, (b) HNO_3, and (c) *aqua regia* as solvent.

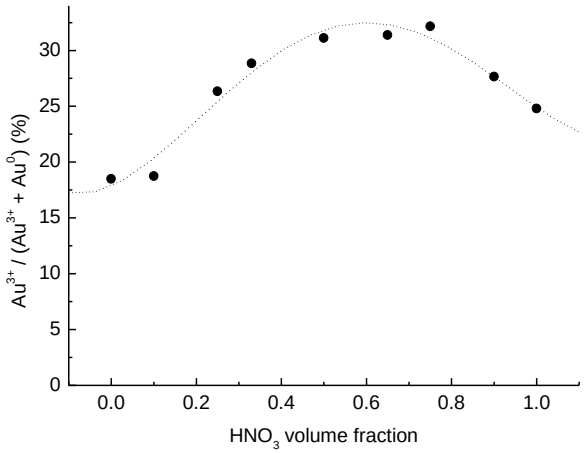

Figure 9. TPR intensities for the reduction of Au^{3+} species for Au/C catalysts prepared using different HNO_3 volume fraction in the HCl:HNO_3 solvent mixture. All catalysts were dried at 140 °C.

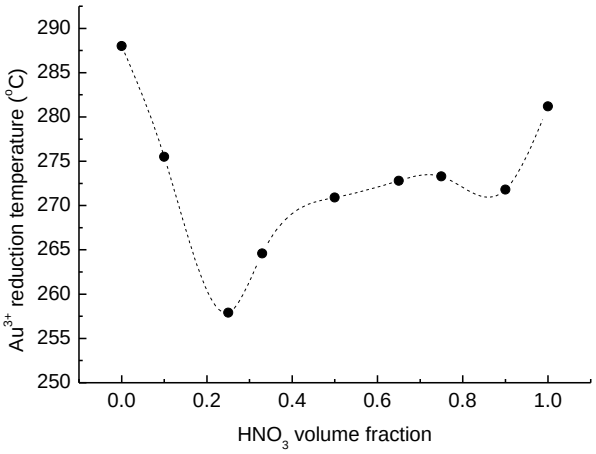

Figure 10. Au^{3+} reduction temperature from temperature programmed reduction in presence of H_2 for Au/C catalysts prepared using different HNO_3 volume fractions in the HCl:HNO_3 solvent mixture. All catalysts were dried at 140 ^oC.

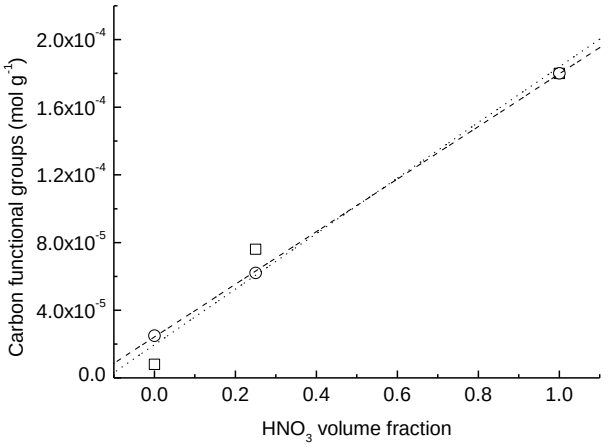

Fig. 11. Oxygenated carbon functional groups (carboxylic/lactones) induced by the presence of HNO_3 in the preparation mixture for HCl, aqua regia, and HNO_3, (○) and (- -) Au/C catalysts, (□) and (··) Au/C catalysts from acid pre-treated carbons.

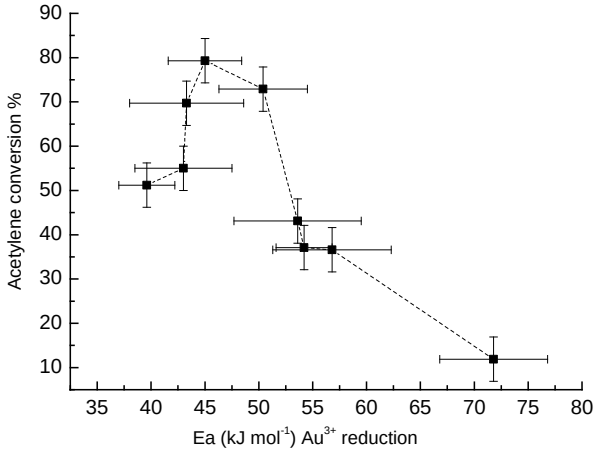

Figure 12. Maximum acetylene conversion (after 5h) versus activation energies for the reduction of Au^{3+} in hydrogen.

Comment [I1]: New plot with error bars

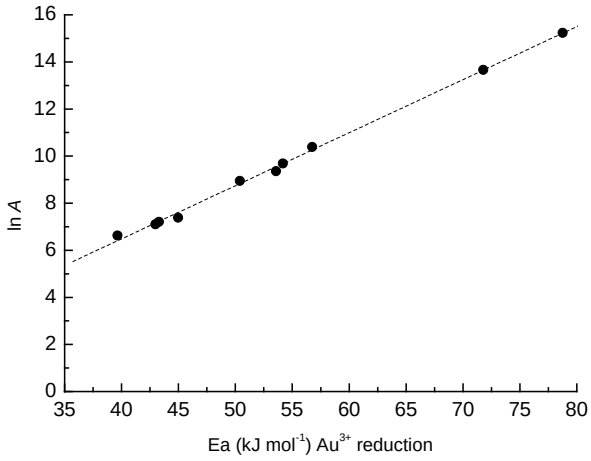

Figure 13. Compensation plot for the reduction of Au^{3+} over Au/C using H_2, for catalysts prepared using HCl, HNO_3 and *aqua regia*, dried at 110, 140 and 180 ^{o}C.